ELECTRONIC SUPPLEMENTARY INFORMATION

Structure-Based Thermodynamics of Ion Selectivity (Mg^{2+} versus Ca^{2+} and K^{+} versus Na^{+}) in the active site of the eukaryotic lariat group II intron from algae *Pylaiella littoralis*

Abhishek Kumar and Priyadarshi Satpati*

Department of Biosciences and Bioengineering, Indian Institute of Technology Guwahati, Guwahati 781039, Assam, India

* Correspondence and requests for materials should be addressed to P.S. (Tel: +91-361-2583205, Fax: +91-361-2582249, e-mail: psatpati@iitg.ac.in)

Table of Contents

Table S1. Details of biomolecular systems considered for classical MD simulations.

System	Number of atoms	Number of water molecules	Number of Divalent ions	Number of Monovalent ions
Pre-hydrolytic (2s) state	47731	14410	25	05
Post-hydrolytic state	47852	14530	14	01

Table S2. Simulation time scale (in *ns*) and estimated free energetics (in kcal mol^{-1}) from the alchemical transformation of $Mg^{2+} \rightarrow Ca^{2+}$, and $K^{+} \rightarrow Na^{+}$ in water (Free) and in complex with lariat group II intron at pre-hydrolytic (2s) and post-hydrolytic state.

Alchemical transformation	System	Replica	MD Free energy calculations Time (ns)	Estimated ΔG (kcal mol^{-1})
$Mg^{2+} \rightarrow Ca^{2+}$	Free in water	Replica 1	22	68.90 (0.41)
		Replica 2	22	68.83 (0.56)
		Replica 3	22	68.64 (0.62)
		Replica 4	22	68.69 (0.67)
		Replica 5	22	68.81 (0.49)
			Average	**68.77 ±0.11**
	Pre-hydrolytic (2s) state	Replica 1	22	150.56 (1.57)
		Replica 2	22	150.38 (1.52)
		Replica 3	22	150.74 (1.67)
		Replica 4	22	150.22 (2.23)
		Replica 5	22	151.68 (1.10)
		Replica 6	22	151.52 (0.79)
			Average	**150.85 (0.61)**
	Post-hydrolytic state	Replica 1	22	156.45 (1.78)
		Replica 2	22	157.69 (1.40)
		Replica 3	22	155.18 (2.56)
		Replica 4	22	158.53 (1.57)
		Replica 5	22	157.91 (1.41)
		Replica 6	22	157.88 (1.56)
			Average	**157.27 (1.23)**
	Free in water	Replica 1	22	-23.47 (0.41)
		Replica 2	22	-23.45 (0.35)
		Replica 3	22	-23.36 (0.56)
		Replica 4	22	-23.28 (0.28)
		Replica 5	22	-23.51 (0.37)
			Average	**-23.41 (0.09)**
		Replica 1	22	-22.53 (0.72)
		Replica 2	22	-20.09 (0.41)
		Replica 3	22	-21.57 (0.55)
		Replica 4	22	-20.61 (1.56)

$K^+ \rightarrow Na^+$	Pre-hydrolytic (2s) state	Replica 5	22	-21.49 (0.38)
		Replica 6	22	-22.40 (0.77)
			Average	**-21.45 (0.96)**
	Post-hydrolytic state	Replica 1	22	-23.56 (0.98)
		Replica 2	22	-22.84 (0.94)
		Replica 3	22	-22.90 (1.43)
		Replica 4	22	-25.77 (1.08)
		Replica 5	22	-25.37 (1.15)
		Replica 6	22	-24.35 (0.56)
			Average	**-24.13 (1.25)**

Table S3. Alchemical coordinate λ was defined that connects end states, i.e., λ =1 corresponds to Mg^{2+}/K^+, and λ =0 corresponds to Ca^{2+}/Na^+. Free energy derivative $\partial G/\partial\lambda$ was calculated for alchemical transformation $Mg^{2+} \rightarrow Ca^{2+}/K^+ \rightarrow Na^+$ for 11λ points between 1 and 0. Free energy derivative was calculated as $\partial G/\partial\lambda = \langle U(\lambda=1) - U(\lambda=1)\rangle_\lambda$, where < > represents averaging over MD trajectory at a specific value of λ. Alchemical transformation associated free energies (in kcal mol^{-1}) was calculated by numerically integrating $\partial G/\partial\lambda$ vs λ plot. The MD trajectories were divided into two equal halves and the difference between the computed $\partial G/\partial\lambda$'s from the two halves is reported as uncertainty in the parenthesis at each λ point. Derivative at each λ is given below:

$Mg^{2+} \rightarrow Ca^{2+}$ free in water

λ	**Replica 1**	**Replica 2**	**Replica 3**	**Replica 4**	**Replica 5**
1.00	-154.32 (0.71)	-155.68 (0.08)	-154.70 (0.53)	-154.85 (0.80)	-154.39 (1.78)
0.90	-122.17 (0.07)	-121.06 (1.49)	-121.23 (0.73)	-121.03 (1.34)	-121.43 (0.32)
0.80	-100.19 (1.13)	-99.68 (0.81)	-100.28 (0.08)	-99.83 (0.92)	-100.40 (0.10)
0.70	-84.15 (0.54)	-84.29 (0.36)	-83.57 (0.01)	-84.65 (0.40)	-84.29 (0.34)
0.60	-71.84 (0.67)	-72.20 (0.27)	-71.67 (0.01)	-72.30 (1.51)	-71.62 (0.46)
0.50	-62.06 (0.40)	-61.58 (0.72)	-61.76 (0.14)	-61.75 (0.58)	-61.55 (0.90)
0.40	-53.75 (0.95)	-53.00 (0.62)	-52.40 (2.23)	-52.69 (1.68)	-53.13 (0.08)
0.30	-44.51 (1.38)	-45.29 (0.74)	-45.04 (0.72)	-44.16 (0.90)	-45.47 (0.20)
0.20	-34.47 (0.15)	-34.13 (1.97)	-34.11 (0.56)	-34.65 (2.56)	-34.70 (0.35)
0.10	-26.93 (0.24)	-27.41 (0.26)	-27.44 (0.44)	-26.79 (0.33)	-26.77 (0.29)
0.00	-23.55 (0.43)	-23.64 (0.63)	-23.17 (0.40)	-23.30 (0.50)	-23.09 (0.36)
ΔG	**68.90 (0.41)**	**68.83 (0.56)**	**68.64 (0.62)**	**68.69 (0.67)**	**68.81 (0.49)**

$Mg^{2+} \rightarrow Ca^{2+}$ pre-hydrolytic (2s) state

λ	**Replica 1**	**Replica 2**	**Replica 3**	**Replica 4**	**Replica 5**	**Replica 6**
1.00	-335.63 (3.37)	-335.68 (5.39)	-334.78 (3.67)	-338.06 (7.88)	-340.30 (0.38)	-352.04 (0.76)
0.90	-257.91 (3.01)	-257.09 (2.04)	-261.65 (2.03)	-256.23 (3.94)	-261.06 (0.39)	-260.39 (2.40)
0.80	-210.25 (0.62)	-212.41 (2.59)	-215.20 (0.78)	-210.22 (0.71)	-214.50 (0.29)	-213.68 (1.72)
0.70	-174.19 (0.49)	-180.32 (0.51)	-179.85 (2.47)	-174.01 (0.28)	-181.21 (1.66)	-178.65 (0.60)
0.60	-150.06 (1.75)	-150.73 (0.96)	-149.41 (5.45)	-150.70 (0.67)	-151.32 (2.33)	-153.47 (0.12)
0.50	-129.55 (1.46)	-130.64 (0.65)	-127.41 (1.80)	-129.31 (0.86)	-132.07 (0.89)	-132.65 (1.23)
0.40	-115.88 (0.26)	-114.35 (0.73)	-109.92 (0.20)	-110.80 (1.10)	-113.77 (0.00)	-112.11 (0.31)
0.30	-101.74 (0.39)	-93.27 (2.35)	-99.20 (0.53)	-100.43 (1.29)	-100.31 (0.86)	-96.80 (0.07)
0.20	-88.25 (0.25)	-86.26 (0.09)	-86.93 (0.50)	-89.29 (0.42)	-86.81 (1.48)	-84.47 (0.36)
0.10	-76.86 (1.60)	-77.43 (0.31)	-76.60 (0.61)	-79.08 (1.14)	-75.45 (1.33)	-74.16 (0.49)
0.00	-66.20 (4.13)	-66.91 (1.14)	-67.54 (0.36)	-66.21 (6.22)	-60.13 (2.50)	-65.60 (0.68)
ΔG	**150.56 (1.57)**	**150.38 (1.52)**	**150.74 (1.67)**	**150.22 (2.23)**	**151.68 (1.10)**	**151.52 (0.79)**

Mg^{2+}→Ca^{2+} post-hydrolytic state

λ	Replica 1	Replica 2	Replica 3	Replica 4	Replica 5	Replica 6
1.00	-367.73 (2.92)	-367.97 (4.29)	-375.10 (2.43)	-373.72 (3.58)	-365.99 (2.08)	-355.53 (4.87)
0.90	-277.77 (1.59)	-278.79 (0.86)	-284.41 (2.30)	-279.84 (0.08)	-277.56 (0.46)	-275.85 (0.77)
0.80	-224.61 (4.11)	-224.59 (1.26)	-229.78 (2.72)	-226.46 (0.28)	-226.29 (2.52)	-223.92 (1.85)
0.70	-187.08 (1.76)	-188.54 (2.11)	-173.30 (4.17)	-189.90 (0.47)	-188.32 (0.11)	-185.83 (3.30)
0.60	-159.54 (2.00)	-160.21 (0.63)	-146.71 (1.31)	-159.40 (1.92)	-160.00 (1.31)	-158.89 (0.89)
0.50	-135.76 (2.11)	-136.91 (0.45)	-130.55 (2.41)	-135.63 (0.91)	-138.28 (0.04)	-137.04 (1.37)
0.40	-115.40 (0.47)	-117.41 (0.59)	-113.34 (4.45)	-118.19 (1.10)	-117.55 (0.15)	-116.73 (1.30)
0.30	-100.35 (2.27)	-98.72 (3.56)	-94.73 (2.77)	-97.85 (5.29)	-103.04 (1.42)	-102.22 (0.91)
0.20	-79.69 (0.43)	-83.83 (0.69)	-85.22 (4.70)	-84.10 (0.47)	-80.14 (1.84)	-89.60 (0.84)
0.10	-70.82 (1.05)	-72.03 (0.16)	-74.38 (0.83)	-74.02 (1.08)	-74.78 (2.52)	-77.41 (0.68)
0.00	-59.20 (0.92)	-63.65 (0.77)	-63.60 (0.10)	-65.94 (2.05)	-60.13 (3.11)	-67.12 (0.38)
ΔG	**156.45 (1.78)**	**157.69 (1.40)**	**155.18 (2.56)**	**158.53 (1.57)**	**157.91 (1.41)**	**157.88 (1.56)**

K^{+}→Na^{+} free in water

λ	Replica 1	Replica 2	Replica 3	Replica 4	Replica 5
1.00	07.25 (0.06)	07.12 (0.20)	07.28 (0.02)	07.28 (0.27)	07.20 (0.12)
0.90	08.97 (0.22)	08.95 (0.06)	08.78 (0.19)	08.91 (0.02)	08.98 (0.23)
0.80	10.52 (0.00)	11.05 (0.22)	10.95 (0.07)	10.80 (0.36)	11.05 (0.30)
0.70	13.23 (0.11)	13.60 (0.31)	13.33 (0.33)	13.63 (0.00)	13.17 (0.70)
0.60	16.49 (0.11)	16.41 (0.31)	16.46 (0.71)	15.99 (0.38)	16.12 (0.21)
0.50	20.00 (0.29)	20.23 (0.90)	20.01 (0.18)	19.89 (0.02)	20.25 (0.22)
0.40	24.41 (0.32)	24.24 (0.19)	24.19 (1.02)	24.12 (0.70)	24.52 (0.24)
0.30	29.87 (1.23)	29.76 (0.00)	29.17 (0.00)	30.11 (0.56)	30.40 (0.62)
0.20	36.35 (0.28)	35.90 (0.10)	36.24 (0.38)	35.08 (0.28)	36.34 (0.90)
0.10	44.38 (1.72)	44.27 (0.88)	43.91 (1.35)	43.88 (0.52)	43.88 (0.52)
0.00	53.73 (0.24)	53.01 (0.75)	53.92 (2.01)	53.56 (0.02)	53.59 (0.02)
ΔG	**-23.47 (0.42)**	**-23.45 (0.36)**	**-23.36 (0.57)**	**-23.28 (0.28)**	**-23.51 (0.37)**

K^{+}→Na^{+} pre-hydrolytic (2s) state

λ	Replica 1	Replica 2	Replica 3	Replica 4	Replica 5	Replica 6
1.00	6.27 (0.07)	6.75 (0.19)	6.67 (1.12)	4.47 (0.28)	6.38 (0.06)	6.17 (0.18)
0.90	7.39 (0.30)	8.11 (0.31)	7.11 (0.26)	6.08 (1.80)	7.38 (0.61)	7.71 (0.38)
0.80	11.02 (0.60)	10.12 (0.26)	8.69 (0.78)	7.00 (1.27)	11.59 (0.17)	10.42 (0.22)
0.70	13.31 (0.45)	14.51 (0.45)	10.75 (0.01)	8.51 (1.29)	13.03 (0.33)	12.32 (0.63)
0.60	16.87 (0.21)	16.33 (0.29)	15.01 (0.01)	9.55 (0.51)	14.36 (0.02)	14.96 (0.10)
0.50	21.51 (0.22)	18.27 (0.74)	19.71 (0.30)	22.38 (0.88)	14.84 (0.03)	18.95 (0.20)
0.40	23.27 (0.06)	21.43 (0.04)	22.35 (0.64)	26.24 (0.80)	22.96 (0.94)	26.38 (0.72)
0.30	27.62 (2.63)	24.49 (0.14)	27.57 (0.03)	28.47 (1.74)	27.91 (0.74)	30.06 (1.20)
0.20	35.50 (0.88)	29.81 (0.85)	34.31 (0.71)	30.67 (2.27)	34.99 (0.96)	37.32 (1.38)
0.10	41.11 (0.50)	33.07 (0.15)	41.65 (0.03)	39.90 (0.44)	39.41 (0.17)	37.97 (1.81)
0.00	48.99 (2.03)	42.81 (1.11)	50.26 (2.18)	50.02 (5.90)	50.32 (0.13)	49.50 (1.70)
ΔG	**-22.53 (0.72)**	**-20.09 (0.41)**	**-21.57 (0.55)**	**-20.61 (1.56)**	**-21.49 (0.38)**	**-22.40 (0.77)**

K^{+}→Na^{+} post-hydrolytic state

λ	Replica 1	Replica 2	Replica 3	Replica 4	Replica 5	Replica 6
1.00	7.88 (0.18)	7.07 (0.26)	7.58 (0.33)	7.46 (0.37)	6.33 (0.30)	7.38 (0.17)
0.90	9.15 (0.76)	8.43 (0.68)	8.00 (0.42)	9.90 (0.99)	8.05 (0.69)	9.01 (0.79)
0.80	11.05 (1.37)	10.75 (0.57)	10.29 (0.02)	11.75(0.14)	10.25 (0.68)	11.50 (0.29)
0.70	13.87 (2.68)	12.67 (0.10)	12.71 (0.70)	14.72 (1.62)	14.54 (1.16)	13.93 (0.03)

0.60	17.70 (0.97)	16.23 (0.31)	16.00 (1.00)	18.38 (0.91)	16.09 (0.22)	17.18 (0.78)
0.50	21.06 (1.59)	18.63 (1.95)	19.36 (2.52)	22.13 (0.54)	25.92 (0.38)	19.89 (0.21)
0.40	25.28 (0.06)	24.49 (0.86)	25.24 (0.60)	24.69 (1.52)	27.89 (2.82)	24.83 (0.46)
0.30	28.87 (0.94)	29.05 (0.35)	28.34 (3.21)	30.98 (0.18)	34.26 (1.74)	29.03 (0.39)
0.20	36.37 (0.26)	35.28 (1.44)	36.21 (0.32)	41.10 (0.81)	34.32 (0.04)	37.38 (1.12)
0.10	42.87 (0.80)	42.34 (0.86)	42.53 (1.07)	50.41 (1.86)	49.84 (3.13)	48.47 (0.76)
0.00	50.81 (0.37)	54.01 (2.99)	52.94 (5.54)	59.71 (2.97)	58.60 (1.51)	57.03 (1.16)
ΔG	**-23.56 (0.98)**	**-22.84 (0.94)**	**-22.90 (1.43)**	**-25.77 (1.08)**	**-25.37 (1.15)**	**-24.35 (0.56)**

Table S4. Estimated Mg^{2+} vs. Ca^{2+} and K^{+} vs. Na^{+} relative binding free energy (**ΔΔG** in kcal mol^{-1}, averaged from various MD runs) to the lariat group II intron active site.

Alchemical path	**State**	**ΔG_{Comp}**	**ΔG_{free}**	**ΔΔG (kcal mol^{-1})**
$Mg^{2+} \rightarrow Ca^{2+}$	Pre-hydrolytic (2s) state	150.85 ± 0.61	137.64 ± 0.13	13.21 ± 0.62
	Post-hydrolytic state	157.57 ± 1.23		19.93 ± 1.24
$K^{+} \rightarrow Na^{+}$	Pre-hydrolytic (2s) state	-21.45 ± 0.96	- 23.41 ± 0.09	-1.96 ± 0.96
	Post-hydrolytic state	-24.13 ± 1.25		0.72 ± 1.25

Alchemical path **CHARMM27 Force-field**	**State**	**ΔG_{Comp}** *(Averaged over two replicas)*	**ΔG_{free}** *(Averaged over two replicas)*	**ΔΔG (kcal mol^{-1}) [CHARMM27 Force-field]**
$Mg^{2+} \rightarrow Ca^{2+}$	Pre-hydrolytic (2s) state	151.54 ± 1.12	137.64 ± 0.02	13.9 ± 1.12

Table S5. Single point energies estimated from quantum chemical calculations for lariat group II intron at pre-hydrolytic (2s) and post-hydrolytic state. The free state was obtained by deleting the RNA part, thus, the solvation shells of the ions were incomplete in the modeled free state.

System	Theory	Snap	Energy (in **hartree**)				E4+E3-(E1+E2)*627.5095 = **ΔE** **(in kcal mol^{-1})**
			(E1) [Mg^{2+}-Wat]	(E2) E2:[Ca^{2+}-intron]	(E3) E3:[Ca^{2+}- Wat]	(E4) [Mg^{2+}-intron]	
Pre-hydrolytic (2s)	B3LYP/6-31+G*	1	-934.886655	-7330.8419777	-1890.0082931	-6375.8670408	-92.06
		2	-934.8676079	-7330.8572319	-1889.9911469	-6375.8439611	-69.19
		3	-934.8864372	-7330.8445735	-1890.006156	-6375.8652379	-88.09
		4	-934.8738276	-7330.8378888	-1890.0079453	-6375 .8341293	-81.80
		5	-934.8794103	-7330.8388081	-1890.00974	-6375.8689337	-100.69
							Average = -86.37 ± 11.79
	MO62X/6-31++G**	1	-934.853335	-7330.4940373	-1890.097316	-6375.4307981	-113.42
		2	-934.8347766	-7330.5237078	-1890.0882697	-6375.3935263	-77.38
		3	-934.8520294	-7330.5077563	-1890.0991663	-6375.4114539	-94.65
		4	-934.8376996	-7330.4996245	-1890.0985329	-6375.3780508	-87.39
		5	-934.8474341	-7330.5198461	-1890.0980402	-6375.4103753	-88.56
							Average = -92.28 ± 13.34
Post-hydrolytic	B3LYP/6-31+G*	1	-858.4427933	-8205.5691657	-1813.5849262	-7250.6012951	-109.35
		2	-858.442724	-8205.5652466	-1813.5709949	-7250.5621825	-78.57
		3	-858.4327475	-8205.5729735	-1813.5760631	-7250.5486238	-74.65
		4	-858.4349697	-8205.5587776	-1813.5776324	-7250.6073027	-119.97
		5	-858.4341287	-8205.5676876	-1813.5755625	-7250.5728078	-91.96
							Average = -94.90 ± 19.51
	MO62X/6-31++G**	1	-858.3989058	-8205.2012593	-1813.6643282	-7250.0982393	-101.91
		2	-858.3989334	-8205.2041156	-1813.6535683	-7250.0683153	-74.57
		3	-858.3902645	-8205.213749	-1813.6574403	-7250.0408083	-59.13
		4	-858.3908214	-8205.2120212	-1813.658209	-7250.1213082	-110.86
		5	-858.3924048	-8205.2041254	-1813.6574645	-7250.0759797	-85.91
							Average = -86.48 ± 20.75

Table S6. Comparison of estimated ΔE for two free state models (incomplete solvation and complete solvation models). Explicit solvation model of the metal ions in the free state (**red bold**). ΔE depends on the solvation model of the ions in the free state. The negative sign of ΔE confirms that Mg^{2+} is preferred over Ca^{2+} in the lariat intron binding pocket. The explicit solvation model of the free Mg^{2+} included six water molecules from the first shell coordination sphere and another water molecule from 2nd coordination shell. The explicit solvation model of the free Ca^{2+} included first shell coordination (i.e., seven water molecules).Ten representative snapshots are taken from the MD trajectories and averaged for estimating ΔE (4^{th} column).

System	Theory	ΔE (in kcal mol^{-1})	
		Incomplete solvation shell in the free state	**Complete solvation shell in the free state**
Pre-hydrolytic (2s) state	B3LYP/6-31+G*	-86.37	**-11.35**
	MO62X/6-31++G**	-92.28	**-20.67**
Post-hydrolytic state	B3LYP/6-31+G*	-94.90	**-12.17**
	MO62X/6-31++G**	-86.48	**-6.89**

Table S7. Intron and ion were described as a single dielectric medium with a dielectric constant of 2 or 4; solvent was treated as another structure-less medium with a dielectric constant of 80. The boundary between the low and high dielectric media was computed with a probe sphere of radius 2 Å. The system was discretized using a cubic grid with 163 regularly spaced planes and a spacing of 1 Å. The ionic strength in the aqueous medium was set to 0.15 M. The Poisson equation was solved numerically using the PBEQ module of the CHARMM program. 1000 snaps with 2 ps interval from the MD trajectories of the end states (alchemical simulation) were used for estimating the electrostatic solvation free energy associated with divalent metal ion binding to lariat intron (ΔG_{PB}). Negative ΔG_{PB} indicated favorable ion binding; magnitude indicated Mg^{2+} binding to the lariat-intron is favored relative to Ca^{2+}.

State	Mg^{2+} , Mg^{2+}-binding to Lariat **ΔG_{PB}^{Mg2+} in kcal/mol**	Ca^{2+} , Ca^{2+} -binding to Lariat **ΔG_{PB}^{Ca2+} in kcal/mol**
Pre-hydrolytic state	($\epsilon = 2$) -96.85 ± 9.40 ($\epsilon = 4$) -87.42 ± 5.44	($\epsilon = 2$) -19.88 ± 10.51 ($\epsilon = 4$) -47.88 ± 5.91
Post-hydrolytic state	($\epsilon = 2$) -96.55 ± 10.33 ($\epsilon = 4$) -82.21 ± 5.28	($\epsilon = 2$) -28.71 ± 9.34 ($\epsilon = 4$) -47.30 ± 4.78

Figure S1. MD simulation setup: Truncated model of 25Å radii sphere centered at P atom of the residue ADE 574 of lariat group II intron was considered for MD simulations. Heavy atoms of the "buffer region" (22Å-25Å) were harmonically restrained to their experimentally determined positions, and a water box of edge length 80Å was overlaid. The solvated truncated model was then subjected to minimization, equilibration, production MD, followed by alchemical free energy calculations.

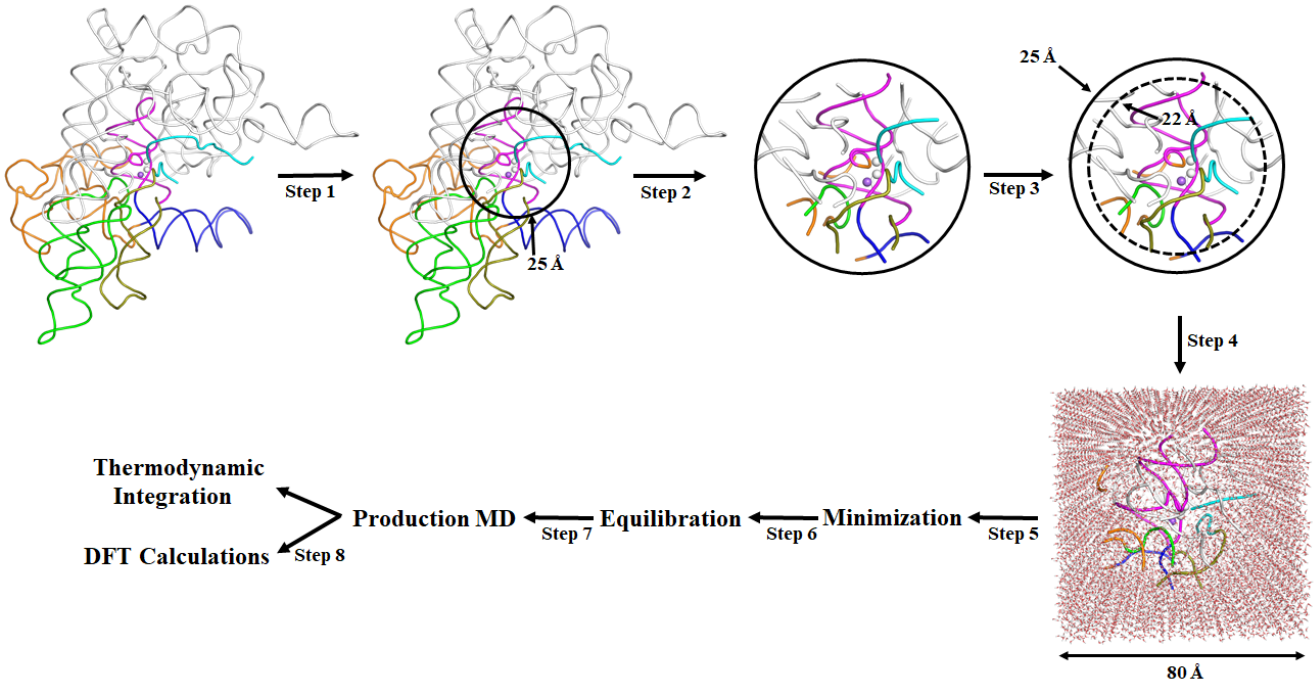

Figure S2. Binding pocket models (M1, M2 site) were considered for quantum chemical calculations. (a,b) Pre-hydrolytic (2s) state (c,d) Post-hydrolytic state. Nucleotide bases were replaced by the methyl group. Mg^{2+} in white sphere and Ca^{2+} in cyan sphere.

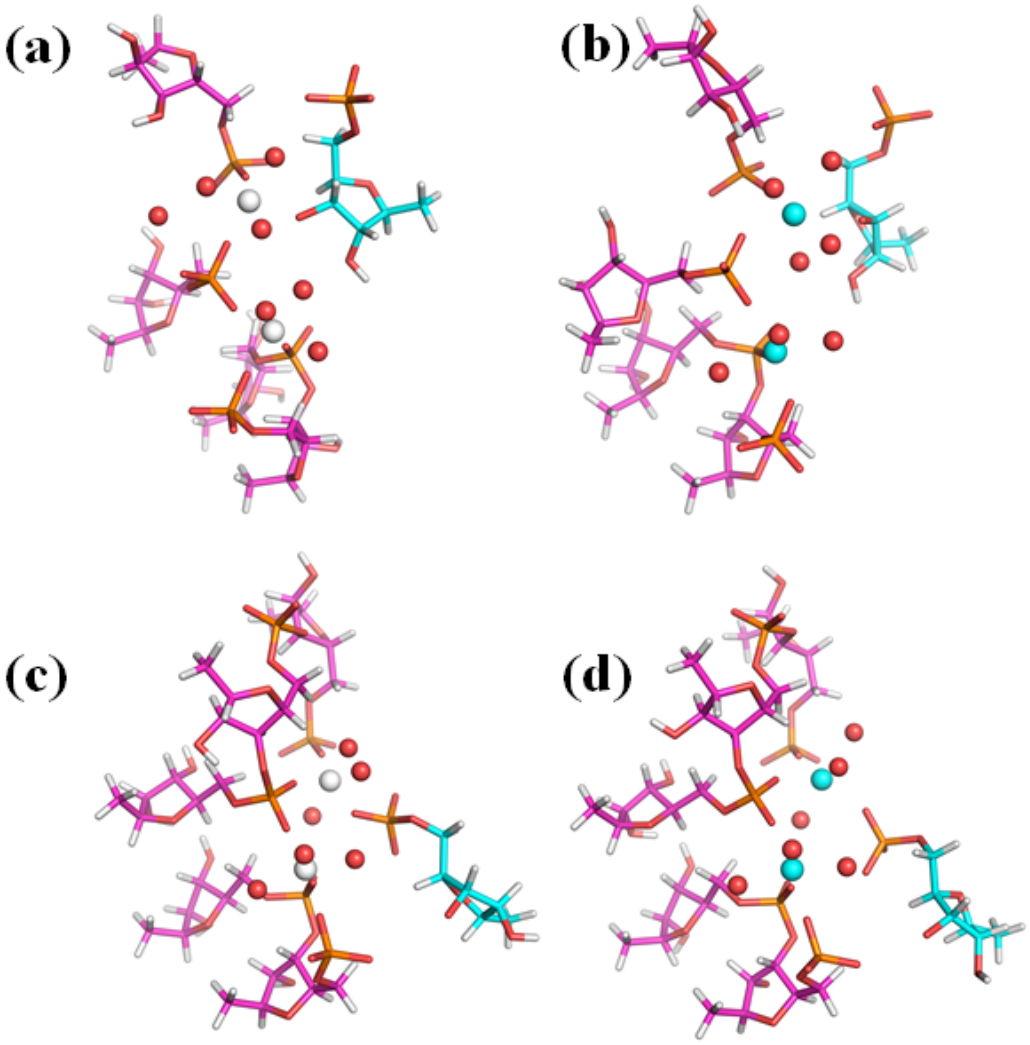

Figure S3. RMSD vs. Time plot from 100ns trajectory: (a) Root-mean-square deviation of heavy atoms within 22Å radius of the active site pocket of lariat group II intron relative to template X-ray structures. Pre-hydrolytic (2s) (black), post-hydrolytic (red). Structural comparison [MD (coloured) and X-ray (Grey)]: (b) Pre-hydrolytic (2s), (c) post-hydrolytic. The non-hydrogen atoms of the RNA in the "buffer region" (22-25Å from the centre) were harmonically restrained to their experimentally resolved positions. Thus, RMSD estimation, including the buffer region, will bias the result by reducing the overall structural deviation between the MD and template structure. Thus, we reported RMSD excluding the portions of the backbone that are harmonically restrained (buffer region).

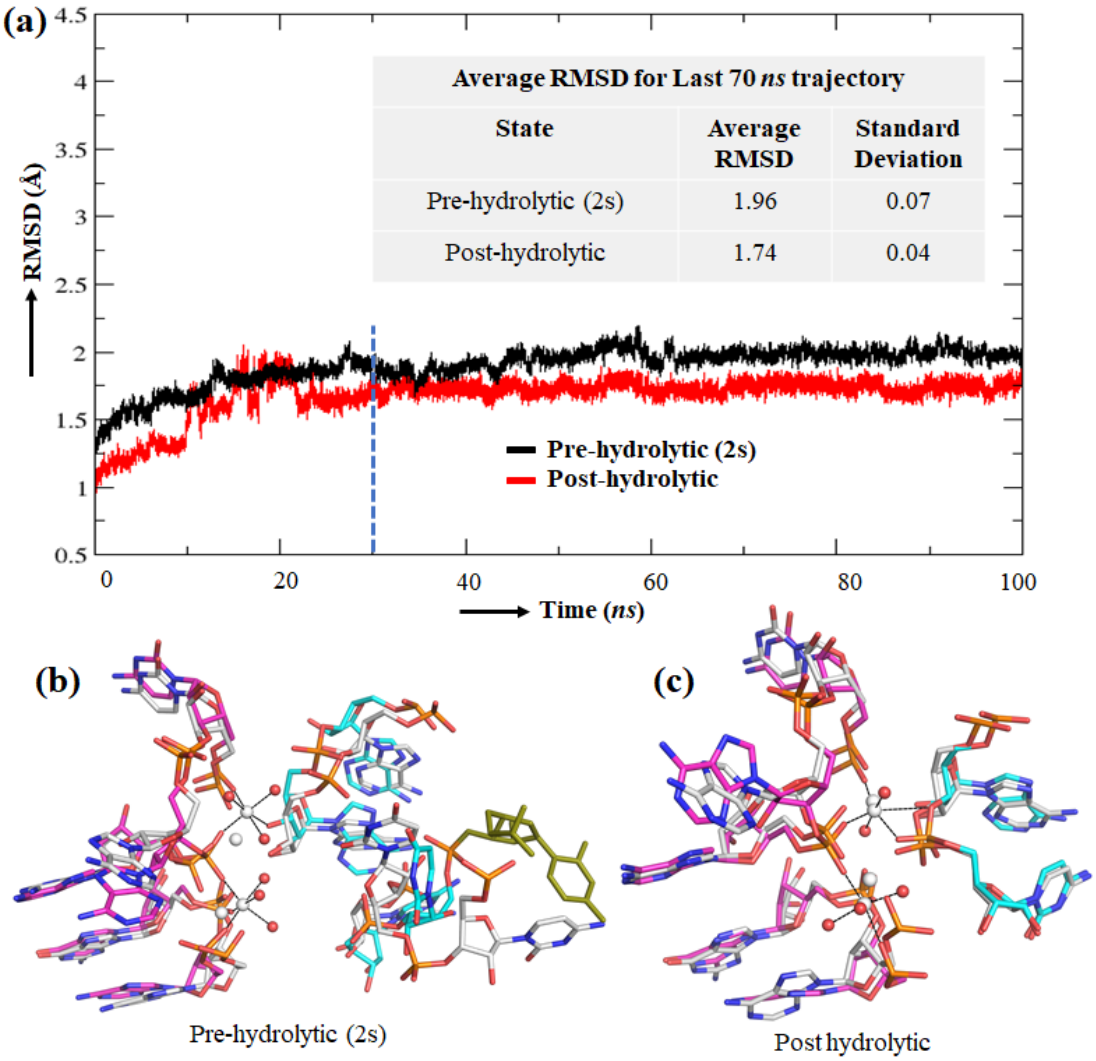

Figure S4. Root-mean-square fluctuation (RMSF) of the heavy atoms of RNA nucleotides of lariat group II introns. Average RMSF was computed from the last 50 ns of post equilibrated MD trajectory. Right-side (exon-part) and left-side (intron-part) of vertical line (black line). The metal-ion binding pocket residues are marked with black/red arrows.

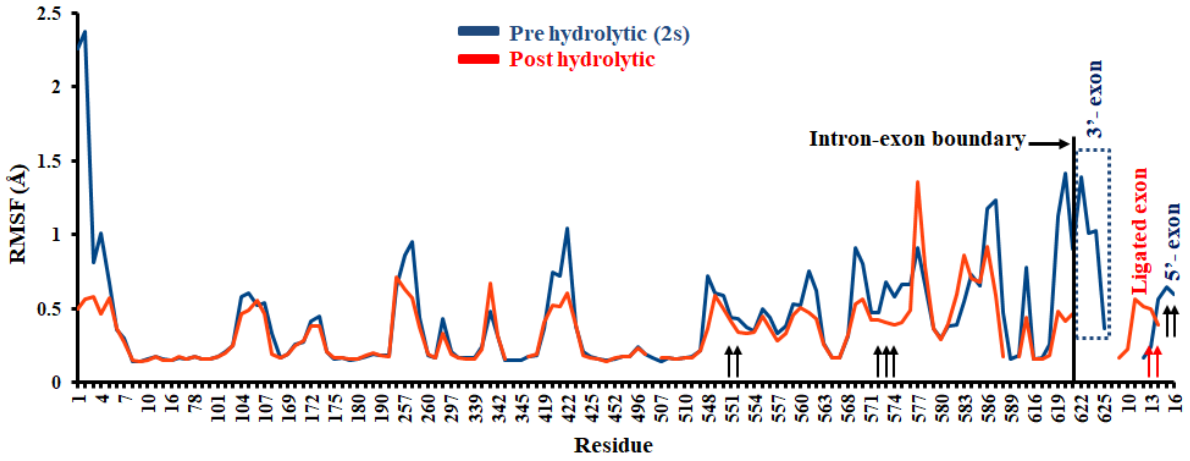

Figure S5. MD structures of the K1 binding pocket in the pre-hydrolytic (2s) state from six independent MD runs. Left (K^+ bound), Right (Na^+ bound)

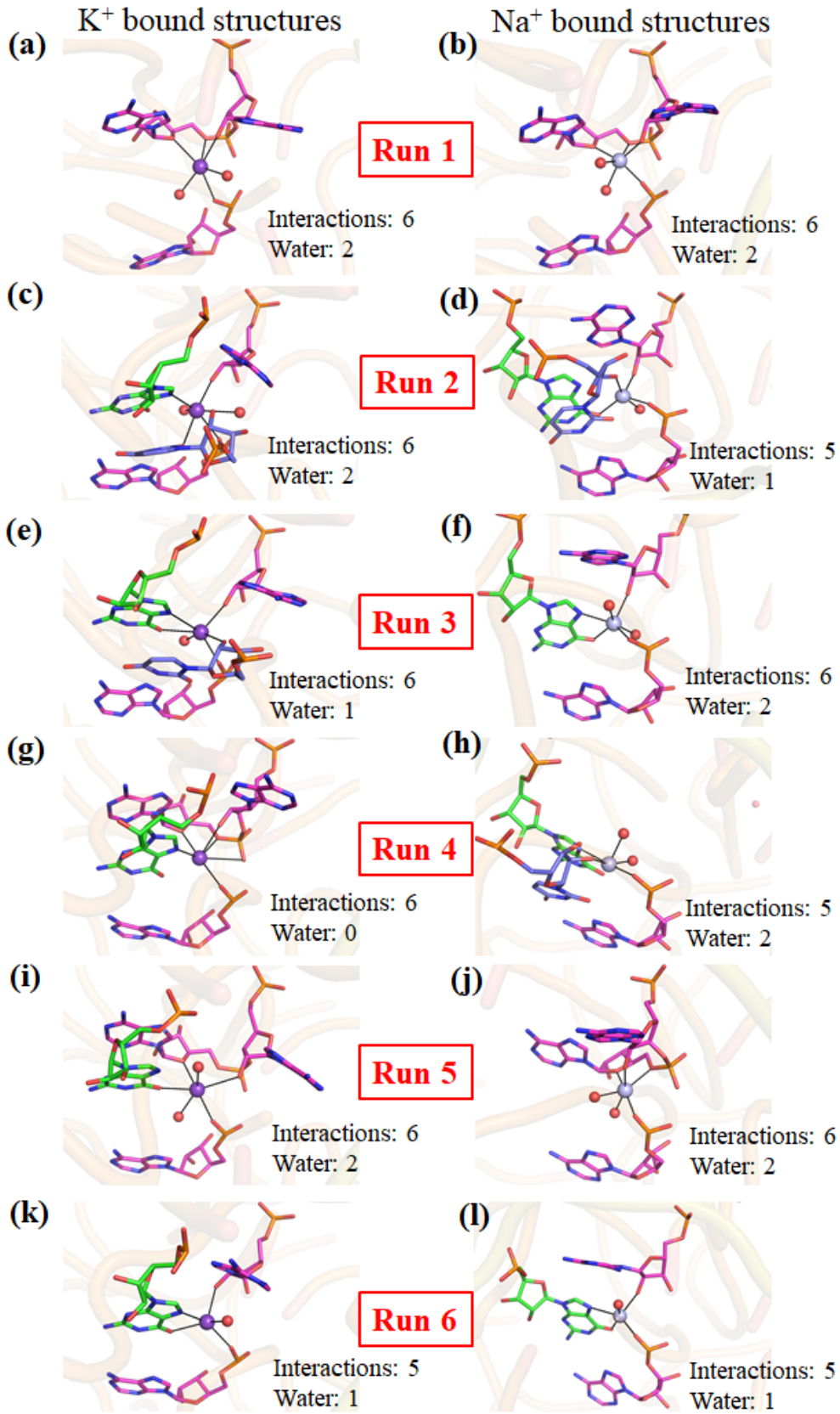

Figure S6. MD structures of the K1 binding pocket in the post-hydrolytic state from five independent MD runs. Left (K^+ bound), Right (Na^+ bound)